Temperature fluctuations and the thermodynamic determination of the cooperativity length in glass forming liquids

Y. Z. Chua, R. Zorn, O. Holderer, J. W. P. Schmelzer, C. Schick, and E. Donth

Citation: The Journal of Chemical Physics **146**, 104501 (2017); doi: 10.1063/1.4977737
View online: http://dx.doi.org/10.1063/1.4977737
View Table of Contents: http://aip.scitation.org/toc/jcp/146/10
Published by the American Institute of Physics

Temperature fluctuations and the thermodynamic determination of the cooperativity length in glass forming liquids

Y. Z. Chua,[1,2] R. Zorn,[3] O. Holderer,[4] J. W. P. Schmelzer,[1,2] C. Schick,[1,2,a)] and E. Donth[5]
[1]*Institute of Physics, University of Rostock, Albert-Einstein-Str. 23-24, 18051 Rostock, Germany*
[2]*Competence Centre CALOR, Faculty of Interdisciplinary Research, University of Rostock, Albert-Einstein-Str. 25, 18051 Rostock, Germany*
[3]*Jülich Centre for Neutron Science, Forschungszentrum Jülich, 52425 Jülich, Germany*
[4]*Jülich Centre for Neutron Science (JCNS) at Heinz Maier-Leibnitz Zentrum (MLZ), Forschungszentrum Jülich GmbH, Lichtenbergstr. 1, 85748 Garching, Germany*
[5]*Wachbergstr. 3, 01326 Dresden, Germany*

(Received 5 December 2016; accepted 15 February 2017; published online 10 March 2017)

The aim of this paper is to decide which of the two possible thermodynamic expressions for the cooperativity length in glass forming liquids is the correct one. In the derivation of these two expressions, the occurrence of temperature fluctuations in the considered nanoscale subsystems is either included or neglected. Consequently, our analysis gives also an answer to the widely discussed problem whether temperature fluctuations have to be generally accounted for in thermodynamics or not. To this end, the characteristic length-scales at equal times and temperatures for propylene glycol were determined independently from AC calorimetry in both the above specified ways and from quasielastic neutron scattering (QENS), and compared. The result shows that the cooperative length determined from QENS coincides most consistently with the cooperativity length determined from AC calorimetry measurements for the case that the effect of temperature fluctuations is incorporated in the description. This conclusion indicates that—accounting for temperature fluctuations—the characteristic length can be derived by thermodynamic considerations from the specific parameters of the liquid at glass transition and that temperature does fluctuate in small systems. *Published by AIP Publishing.* [http://dx.doi.org/10.1063/1.4977737]

I. INTRODUCTION

Thermodynamics and its statistical mechanical interpretation are originally developed for large (in the limit, infinite) systems.[1–4] When applying thermodynamics to finite equilibrium systems in contact with a thermostat, one has to take into account the increasing role of fluctuations with a decrease of the size of the considered subsystem in the analysis of its properties. As one of the problems, the question occurs regarding the way to determine the state parameters of the system under consideration.

In the determination of the extensive state parameters of the subsystem, such as energy, U, number of particles of the different components, n_i, volume, V, no uncertainties arise. This statement is true also for the set of intensive state parameters, which can be defined as ratios of the above mentioned extensive state parameters, such as the particle density of the different components, n_i/V. The specification of these parameters for the systems under consideration requires multiple measurements with a subsequent averaging over time or the respective ensemble.

The situation is more complicated with respect to the set of intensive state parameters, such as pressure, p, temperature, T, or chemical potentials, μ_i, the definition of which requires from the very beginning some averaging procedure. As even noted by Landau and Lifshitz: "*Temperature is as entropy obviously a quantity of purely statistical character, which has a definite meaning only for macroscopic systems*." (Ref. 4, Chap. 2, paragraph 9.) On the other hand in treating thermal fluctuations, Landau and Lifshitz[4] consider a small closed subsystem in an extended thermostat (cf. also Ref. 5), so the question is obviously how small subsystems can be to be allowed to be treated in such terms.

In analyzing the mentioned class of quantities, on one side, when they are considered formally as unique functions of the state parameters of the system, then they and even their fluctuation characteristics can be easily determined, at least for relatively moderate fluctuations.[1–4] On the other hand, the existence of such fluctuations leads to a variety of problems, for example, how one has to determine the equilibrium conditions (for the average or the most probable values), or whether the macroscopic definitions of these quantities can be retained for small systems (cf. also Refs. 5 and 6).

With respect to temperature, a straightforward resolution of this circle of problems was proposed by Kittel, strictly denying the existence of temperature fluctuations. He wrote "*the energy of the system may fluctuate but the temperature does not*" (Chap. 6, comment to exercise 6.3 in Ref. 3). He retained his point of view also later denoting temperature fluctuations as an oxymoron, i.e., a combination of contradictory words.[7] In contrast, this point of view was heavily opposed by Mandelbrot considering temperature fluctuations as a "*well-defined and unavoidable notion*".[8]

a)Author to whom correspondence should be addressed. Electronic mail: christoph.schick@uni-rostock.de

Indeed, the concept of temperature fluctuations has turned out to be very useful in the interpretation of experimental data.[4,9,10] Moreover, denying of temperature fluctuations but retaining energy fluctuations would lead to a conflict with well-known relations between energy, temperature, and their fluctuations (cf. the paper of von Laue[11] mentioned also by Kittel[12]). However, on the other hand, as shown in detail by McFee[9] (cf. also Ref. 5), for small systems one may arrive—at certain weak assumptions—at the conclusion that the average temperature of small systems in equilibrium with a thermostat is different from the temperature of the thermostat, leading to a severe contradiction between classical thermodynamics (in particular the second law (Carnot's principle[5]) and the zeroth law of thermodynamics[6]) and its statistical mechanical interpretation. For such case, the construction of a perpetuum mobile of second order should be possible, as noted by McFee.[9]

Based on the work, in particular, of Clausius, Maxwell, and Boltzmann, Gibbs[13] analyzed in detail the problem of the derivation of the laws of thermodynamics from the principles of mechanics. He noted in the introduction to his book: "*The laws of thermodynamics, as empirically determined, express the approximate and probable behavior of systems of a great number of particles*," they "*may be easily obtained from the principles of statistical mechanics, of which they are the incomplete expression*." Arriving at relations similar to the combined first and second laws of thermodynamics, an alternative definition of temperature is advanced by him, which for macroscopic systems is equivalent to the thermodynamic definition. It could be denoted as the Boltzmann or Gibbs definition of temperature (cf. also Ref. 8). Gibbs further discussed a variety of problems in this approach, in particular, the non-uniqueness of definition of temperature for systems with a small number of degrees of freedom.

The problem in the difference of the average temperature of a small system from the temperature of the surrounding thermostat[5–7,9] can be resolved by utilizing the basic concepts as developed by Gibbs in the following way (cf. Ref. 5): by employing Gibbs approach to the analysis of a perfect gas and connecting temperature uniquely with energy, for subsystems of any size, the average temperature is equal to the temperature of the thermostat. Determining, in addition, the derivative of entropy with respect to energy for this model system, it can be shown that the thermodynamic definition of temperature becomes applicable only if for the particle numbers the relation $1 >> (2/3N)$ holds.

Concluding these considerations, we come to the conclusion that—as far as the systems are sufficiently large—temperature fluctuations can easily be determined via standard approaches of statistical physics. For smaller systems, the thermodynamic definition may break down and definitions of temperature could be employed instead connecting temperature with energy. Consequently in both cases, temperatures may be considered to be fluctuating without leading to internal contradictions. However, taking into account the wide spectrum of opinions in this respect as discussed above, a direct experimental proof of the question whether temperature fluctuations do exist for small systems or not can be considered to be of outstanding interest.

This circle of problems—does temperature fluctuate or not—was discussed intensively in a series of papers by Donth *et al.*[6,14,15] Experiments have been suggested in the cited references allowing one to assess whether this is the case or not. In particular, it was shown that a decision between the alternatives is possible by a calorimetric determination of the characteristic length of dynamic glass transitions in confined geometries, since the mentioned alternatives result in different formulas for these lengths. Or more recently, it was suggested to compare the characteristic length of glass transition for both cases at time scales of the relaxation at which a length scale is independently available at the same time scale from neutron scattering experiments.[16] Such an experiment is thought to contribute to the two circles of problems: (i) Does temperature fluctuate? and (ii) does the estimate for the characteristic length scale at the glass transition derived by Donth under the assumption of the existence of temperature fluctuations provide realistic values?[17]

To obtain an independent measure of the characteristic length scale from dynamics is often said to require four-point correlation functions. While these are straightforward to calculate from molecular dynamics simulations, cf. Ref. 18, they cannot be obtained experimentally. Nevertheless, recent experiments indicate a way to obtain cooperativity numbers from non-linear susceptibilities.[19,20] But these methods at the moment cannot provide absolute values needed for a quantitative comparison. Here, we propose a different access route and describe how to obtain information about characteristic length of cooperatively rearranging regions (CRR) determined from glass transition dynamics by AC calorimetry in a wide frequency range, as well as by quasielastic neutron scattering (QENS).

Finally we would like to note that in the framework of thermodynamics, one can also study size effects but from a different point of view accounting for the existence of surfaces and specific surface energies. Respective theories have been developed first by Gibbs and, in an alternative continuums approach by van der Waals at the end of the 19th century.[21,22] Another approach has been attempted to be developed by Hill.[23] With respect to the present paper, a discussion of possible advantages of one of these methods is not required since they all discuss problems not relevant for the present research topic.

The paper is structured as follows: First, the AC calorimetric techniques and incoherent neutron spin echo spectroscopy utilized are briefly described. Then results of polystyrene and propylene glycol measured with AC calorimetry, laser-modulated AC calorimetry, and with QENS for propylene glycol will be presented for comparison. Finally, the paper ends with a discussion and conclusion.

II. EXPERIMENTAL STRATEGY

It has been a longstanding question, whether there is a characteristic length associated to the glass transition.[14,17,24] Therefore, the characteristic length, ξ_α, for the dynamic glass transition cooperativity remains widely investigated and a long-running issue despite being still not fully understood. The characteristic length is defined as the size of a CRR for

the α-relaxation, where a subsystem of the sample, which upon a sufficient thermal fluctuation, can rearrange into another configuration independently of its environment. The average size of a CRR is, therefore, determined by a spatial aspect of statistical independence of thermal fluctuations.

The characteristic length of the CRR can be determined from the parameters of the glass transition. The length is expressed by cooperativity, N_α, the number of molecules or monomeric units in a CRR. According to Ref. 15 referring to Refs. 25–27, the formula for the cooperativities, N_α, derived by neglecting temperature fluctuations (energy fluctuations only, $\delta T = 0$), is given by

$$N_\alpha(\delta T = 0) = \frac{RT_\alpha^2}{M_0 \cdot \delta T_g^2} \cdot \frac{1}{\Delta c_v}, \tag{1}$$

while for the case that temperature fluctuations are accounted for, the following relation can be derived:[17]

$$N_\alpha(\delta T) = \frac{RT_\alpha^2}{M_0 \cdot \delta T^2} \cdot \Delta(1/c_v), \tag{2}$$

with $\Delta(1/c_v) = 1/{c_v}^{\text{glass}} - 1/{c_v}^{\text{liquid}}$ the step of reciprocal-specific heat capacity at glass transition, while $\Delta c_v = {c_v}^{\text{liquid}} - {c_v}^{\text{glass}}$. In Equation (1), δT_g is the glass transition temperature distribution of CRRs with different internal configuration, while in Equation (2), δT is the mean temperature fluctuation of the CRRs. Both are assumed to be equal to the half of the full width half maximum (FWHM) of the imaginary part of complex heat capacity of the dynamic glass transition, FWHM = $2\delta T$. T_α is the dynamic glass transition temperature for the frequency, ω, M_0 the molecular weight (for polymers of the repeat unit), and R the universal gas constant.[15,28]

As noted in Ref. 15, only with the determination from the calorimetric glass transition, no *ad hoc* assumptions (besides the decision whether temperature can fluctuate or not) are necessary for the derivation of the characteristic lengths.

Application of AC chip calorimetry extends the accessible frequency range, and was further extended towards much higher frequencies by application of modulated laser light heating, instead of resistive heating. Hence, the characteristic length across a wide temperature range can be determined with calorimetric data in a wide frequency range. Within that approach, the volume of a CRR, V_α, or the characteristic length, ξ_α, of dynamically correlated segments at the glass transition can be calculated according to Equation (2) as

$$\xi_\alpha = \left(\frac{6}{\pi} \cdot V_\alpha\right)^{1/3} \quad \text{with } V_\alpha = \nu_{\text{mol}} N_\alpha \text{ and } \nu_{\text{mol}} = \frac{M_0}{\rho N_A}, \tag{3}$$

where N_A is the Avogadro constant and ρ the density.

Equation (3) depicts the conventional way to determine the length scale in the form of a cooperativity length, ξ_α, by converting the number of cooperatively rearranging molecules, N_α, with the molecular volume into a cooperativity volume, $V_\alpha = \nu_{\text{mol}} N_\alpha$, and subsequently into a length, $\xi_\alpha = (6V_\alpha/\pi)^{1/3}$. Here, we assume that ξ_α is the diameter of a sphere, which will be utilized throughout the paper. Recent experiments by non-linear dielectric spectroscopy confirm that the CRR is a compact three-dimensional region, fixing the exponent to 1/3.[19] The consequence of assuming another shape is discussed below.

It has been suggested by Donth to compare AC calorimetry and QENS, in order to determine the characteristic length in two independent ways. This comparison is usually performed employing approximate relations, which can be justified as order-of-magnitude estimates but not necessarily with the precision required to make an unambiguous decision between the two concepts of the cooperativity length, Equations (1) and (2), to be distinguished. Therefore, we propose a picture enabling a more quantitative comparison.

With AC calorimetry, where we measure complex heat capacity, it is possible to obtain the characteristic frequency, $\omega_{\max}$, of the fluctuations of the entropy relevant for the α-relaxation. In order to assign this characteristic frequency to a length scale, the $\tau_K(Q)$ relation obtained from a neutron scattering experiment is used together with the length scale, which is generally determined as $l = 2\pi/Q^*$. Here Q^* denotes the scattering vector at which, for a given temperature, the time scales of the AC calorimetry experiment and the QENS experiment coincide. Therefore, the equality to be tested in the experiment would be

$$\xi_\alpha = l \approx \frac{2\pi}{Q^*}. \tag{4}$$

The numerator 2π is strictly justified only for the case of a periodic structure, where l signifies a distance of Bragg planes. Indeed in some instances, other factors can be found in the literature, e.g., π as numerator in the case of the determination of particle diameters.[29] In one particular instance, even the relation $l \approx 1/Q^*$ is proposed.[30] Note that all these relations are not derived rigorously from models and theory and thus can only be considered order-of-magnitude estimates. This uncertainty of the estimate of the length scale from the scattering vector of the QENS experiment may not be tolerable for a reliable comparison with the cooperativity length.

In order to reach more quantitative terms, we propose to take the mean-square displacement (MSD) of particles observed by incoherent QENS as a measure of the length scale of the experiment. In the Gaussian approximation, the incoherent intermediate scattering function is related to the MSD as

$$S_{\text{inc}}(Q,t) = \exp\left(-\frac{Q^2 \left\langle r^2(t)\right\rangle}{6}\right). \tag{5}$$

Due to the fitting of the data with the Kohlrausch function, the exponential term becomes −1 when $t = \tau_K$, where τ_K is the Kohlrausch time constant. This leads the MSD at τ_K to be

$$\left\langle r^2(\tau_K)\right\rangle = \frac{6}{Q^{*2}}. \tag{6}$$

To associate this length with the cooperativity length, it seems natural that this quantity corresponds to the average squared distance constructible within the cooperativity volume. As known from the theory of small angle scattering from particles, this average is twice the squared radius of gyration of the volume,

$$\left\langle r^2(\tau_K)\right\rangle = 2R_g^2. \tag{7}$$

Assuming the volume to be spherical, as in Equation (3), the radius of gyration is calculated as

$$R_g{}^2 = \frac{3}{5}R^2 \tag{8}$$

and the volume of a sphere is $V = 4\pi R^3/3$. By combining Equation (6) to the spherical volume, we obtain the correct volume to be compared with the cooperativity volume, V_α from AC calorimetry as

$$V = \frac{20\sqrt{5}\pi}{3Q^{*3}} = \frac{46.8}{Q^{*3}}. \tag{9}$$

Finally since we defined the cooperativity length as the *diameter* of the sphere, the corresponding quantity from the QENS has to be

$$l = 2R \tag{10}$$

and the cooperativity length to be compared with the characteristic length, ξ_α, from AC calorimetry is

$$l = \frac{\sqrt{20}}{Q^*} = \frac{4.47}{Q^*} \tag{11}$$

replacing Equation (4).

Concerning the time scale, the usual relation between frequency and time is $\omega = 1/\tau$. However, even this relation requires some refinement on closer look. In the AC calorimetry experiments performed here, the characteristic frequency, ω_{max}, is the position of the maximum in the imaginary part of complex heat capacity (phase angle), $c_p''(\omega)$. On the other hand, the fits of the neutron spin echo (NSE) data result in the Kohlrausch time constant, τ_K. The (standard) comparison is to associate ω_{max} with the maximum position of the imaginary part of the susceptibility, corresponding to the intermediate scattering function, i.e.,

$$\chi''(Q,\omega) = -\int_0^\infty \frac{d}{dt}\exp\left(-(t/\tau_K)^\beta\right)\sin(\omega t)dt. \tag{12}$$

A numerical determination of the maximum for the value β resulting from our fits gives

$$\omega_{max} = \frac{0.83}{\tau_K} \tag{13}$$

which will be utilized in this paper for the determination of cooperativity length, while acknowledging other possible attributions, which will be presented in Sec. V.

III. EXPERIMENTAL

A. Sample

Atactic polystyrene, PS168N (IUPAC name: poly(1-phenylethene), was purchased from BASF (M_W = 354 kg mol^{-1} and ρ = 1.05 g cm^{-3}), while propylene glycol (IUPAC name: propane-1,2-diol) was purchased from Carl Roth GmbH (M_0 = 76.10 g mol^{-1} and ρ = 1.04 g cm^{-3}). Both samples were used without further purification.

The available dielectric relaxation data[31–33] for a wide frequency range are fitted to the Vogel-Fulcher-Tammann (VFT) equation. From the fit, the glass transition temperature (defined as temperature where $\tau_\alpha(T_g) = 100$ s) of polystyrene is $T_g = 373 \pm 2$ K, while for propylene glycol $T_g = 167 \pm 1$ K. The VFT equation, which represents the temperature dependence of the dielectric relaxation time $\tau_\alpha = 1/(2\pi\nu_{peak})$ accurately, is

$$\log_{10}(\tau_\alpha) = A + \left(\frac{B}{T - T_0}\right) \tag{14}$$

with $A = -10.5$, $B = 475.3$ K, and $T_0 = 334.4$ K for polystyrene, and $A = -14.1$, $B = 881$ K, and $T_0 = 112.5$ K for propylene glycol. The dielectric relaxation data and the fits by the VFT function are displayed in Fig. 12 below. Propylene glycol does not crystallize as it is a racemic mixture, where its stereoisomers are unable to fit into each other.[34] Consequently in our investigation, no crystallization and subsequently no melting of propylene glycol have been observed. The characteristic frequency, $\omega_{max} = 1/\tau_\alpha$, is calculated from the correlation time as in Equation (14), as the average time constant from AC, laser-modulated measurements, and dielectric relaxation data.

Fig. 1 shows the glass and liquid specific heat capacity lines of polystyrene and propylene glycol extrapolated from Refs. 35 and 36, respectively. The specific heat capacity of propylene glycol (solid black squares and line) was measured with (isoperibol) Nernst calorimetry. The specific heat capacity lines of glass and liquid state are fitted with a linear (solid red line) and a polynomial function (solid green line), respectively, and their difference, $\Delta c_p(T)$, changes with temperature. For each temperature, the corresponding $c_p{}^{glass}$ and $c_p{}^{liquid}$ were taken from the curves, in order to determine Δc_p and $\Delta(1/c_p) = 1/c_p{}^{glass} - 1/c_p{}^{liquid}$, for the calculation of characteristic lengths, as mentioned above. However, in order to increase the accuracy of the calculation, c_p is converted to c_v employing

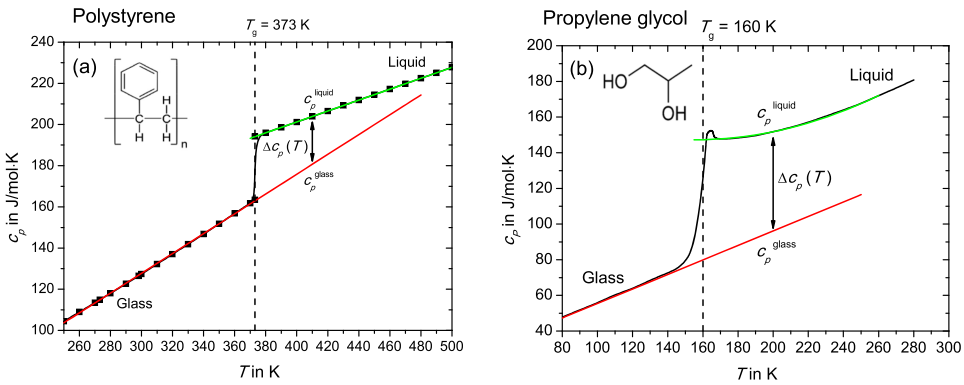

FIG. 1. Specific heat capacity for (a) polystyrene[35] and (b) propylene glycol[36] with adiabatic calorimetry (or Nernst method) from glass to liquid state (solid black squares and line). The specific heat capacity lines of glass and liquid state are extrapolated, as red and green solid lines, respectively. The Δc_p is determined as the difference between $c_p{}^{liquid}$ and $c_p{}^{glass}$ at its respective temperature. The molecular structure of polystyrene and propylene glycol is also included as inset.

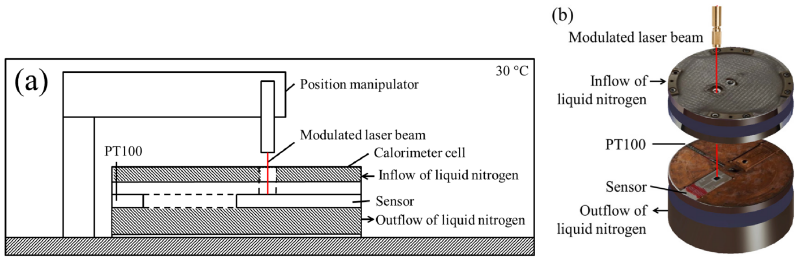

FIG. 2. Schematic of (a) the laser-modulated AC chip calorimeter and (b) the calorimetric cell.

the following equation:

$$c_p - c_v = \frac{M_0 \alpha^2 T}{\rho \beta_T}, \tag{15}$$

where α is the coefficient of thermal expansion, $\beta_T{}^{\text{glass}}$ the isothermal compressibility, and ρ the density. For polystyrene with density, $\rho = 1047$ kg m^{-3}, the coefficients of thermal expansion[37] and isothermal compressibility[38] are $\alpha^{\text{glass}} = 0.75 \times 10^{-4}$ K^{-1} and $\beta_T{}^{\text{glass}} = 1.8 \times 10^{-10}$ Pa^{-1} for glass, and $\alpha^{\text{liquid}} = 2.0 \times 10^{-4}$ K^{-1} and $\beta_T{}^{\text{liquid}} = 3.4 \times 10^{-10}$ Pa^{-1} for liquid, respectively, whereas the coefficients of thermal expansion for glass and liquid of propylene glycol are obtained from Ref. 36, with $\alpha^{\text{glass}} = 2.0 \times 10^{-4}$ K^{-1} and $\alpha^{\text{liquid}} = 6.3 \times 10^{-4}$ K^{-1}. The isothermal compressibility[39] for propylene glycol is $\beta_T = 4.45 \times 10^{-10}$ Pa^{-1} and $\rho = 1040$ kg m^{-3} is the density. The relative difference between c_p and c_v of glass and liquid is about 0.7% and 2.5% for polystyrene and about 1.5% and 7%-10% for propylene glycol, respectively. Even though the difference is small, we employ c_v in our calculation of the characteristic length for better accuracy and consistency.

B. Laser-modulated AC calorimetry

The laser-modulated AC chip calorimetry is similar to that described in detail by Shoifet *et al.*,[40] but was further modified to allow measurements at sub-ambient temperatures. Fig. 2 shows the scheme.

The calorimeter cell was cooled with liquid nitrogen reaching temperatures down to 129 K. In the laser-modulated calorimetry mode, the periodic heating is generated by a modulating laser light with wavelength $\lambda = 675$ nm from a pigtailed laser diode (Thorlabs LPS-675-FC with optical fiber SM600) and the mean temperature scan is controlled by the on-chip resistive heater.

Fig. 3 shows the calorimetric sensor XI274 on the ceramic housing XEN-40014 used for the AC calorimetry and laser-modulated calorimetry measurements in this work. The sensors are chip-nanocalorimeters fabricated by Xensor Integrations, NL.[41] In the laser-modulated calorimetry mode, the glass fiber is first manually positioned as close as possible to the sensor membrane and finally realigned by a three axis electromechanical stage (MP-285, Sutter Instrument, USA) to shine the laser light on top of the sample and the hot junction of the thermocouple, as shown in Fig. 4.

The temperature was calibrated with the plastic crystal I—liquid phase transition of cyclopentane at 178.59 K[42] and dynamic glass transitions of 5-phenyl-4-ether (5PPE).[43]

C. Incoherent neutron spin echo spectroscopy

Neutron scattering offers the unique possibility to observe the dynamics of disordered materials on a microscopic length scale. This is possible because the wavelength of neutrons matches the characteristic intermolecular distance and their energy allows the resolution of energy transfers by the slow process involved at the same time. The scattering function $S(Q, \omega)$, which is basically the probability of scattering dependent on the wave vector, Q, and the energy transfer, $\hbar\omega$, contains the spatial information in the Q dependence and the temporal information in the ω dependence—both in a Fourier transformed representation of the particle correlation function.

Neutron spin echo (NSE) spectroscopy measures directly the *intermediate scattering function*, i.e., the inverse Fourier transform of the scattering function $S(Q, \omega)$ in conventional QENS experiments.[44] In our experiments, due to the high incoherent scattering cross section of protons, the scattering is predominantly incoherent, i.e., from the *self-correlation* of hydrogen nuclei. In the classical approximation, the incoherent intermediate scattering function is directly related to the trajectories of the hydrogen atoms,[45]

$$S_{\text{inc}}(Q, t) = \left\langle \sum_j \exp[\mathbf{Q} \cdot (\mathbf{r}_j(t) - \mathbf{r}_j(0))] \right\rangle. \tag{16}$$

NSE measurements of the incoherent scattering of hydrogen suffer from the problem that the scattering is *spin*-incoherent. This implies that with 2/3 probability, the neutron spin is flipped in the scattering event. This does not preclude NSE experiments, but makes them more difficult in terms of counting statistics.

The NSE experiments were performed on the J-NSE instrument at the neutron source of Heinz Maier-Leibnitz Zentrum, Garching, Germany.[46] For the experiments on polystyrene, all measurements were done using an incident wavelength of 8 Å, except for $Q = 0.15$ Å^{-1} where 10 Å

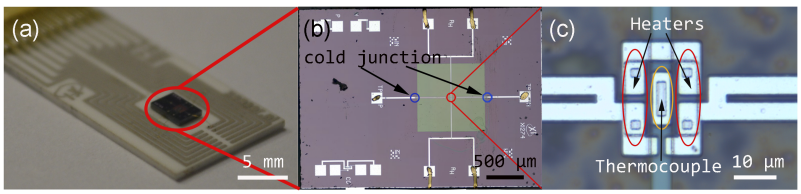

FIG. 3. (a) Calorimetric sensor XI274 on ceramic housing XEN-40014. (b) Enlarged view of the chip with the free-standing SiN_x membrane (green square) and the bond pads (small white squares). (c) The working area with the heater and the thermocouple hot junction. Reproduced with permission from Rev. Sci. Instrum. **84**, 073903 (2013). Copyright 2013 AIP Publishing LLC.

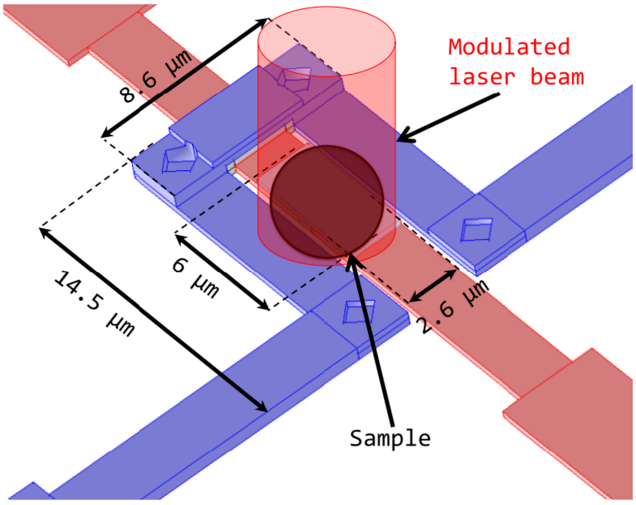

FIG. 4. The position of the modulated laser beam that shines directly only on the sample and on the hot junction of the thermocouple. The two heaters and the aluminum electric connections are shown in blue. The doped poly-Si stripes of the thermocouple are colored in red and the hot junction of the thermocouple, made by an aluminum connection, in gray. Reproduced with permission from Chua *et al.*, Colloid Polym. Sci. **292**, 1893 (2014). Copyright 2014 Springer.

was used. Although the larger wavelength extends the time range from 40 to 75 ns, the measuring time increases drastically. Therefore, this choice was only taken once. While for the experiments on propylene glycol, the incident wavelength was always chosen to be 8 Å, which is close to the optimum flux. At that wavelength, J-NSE allows a measurement of incoherent scattering up to 40 ns at reasonable registration times (about 1 h per Fourier time, half a day for a whole time spectrum at one temperature). The sample was held in an aluminum cuvette with a nominal thickness of 0.34 mm over the complete area of the beam (3 cm × 4 cm). The thickness corresponds to a scattering efficiency of 20%. Due to the partially depolarizing effect of incoherent scattering, the detection of multiple scattering events is strongly reduced.

Neutron spin echo measures directly the normalized intermediate scattering function $S_{\mathrm{inc}}(Q,t)$. In our experiment with propylene glycol, the scattering wave vectors are fixed at values $Q = 1.0$ Å^{-1} and $Q = 1.6$ Å^{-1} for temperatures of 220 K, 230 K, 240 K, and 250 K. For the temperatures of 240 K and 250 K, additional measurements for $Q = 0.6$ Å^{-1} were done to increase the accuracy of the determination of the Q dependence of the relaxation time. Fourier times were chosen in the range between 20 ps and 40 ns, depending on where the data showed significant behavior. The resulting data were interpreted in terms of a model involving two independent relaxation mechanisms, S_{MG} and S_α,

$$S(Q,t) = A(Q,T) \cdot S_{\mathrm{MG}}(Q,t,T) \cdot S_\alpha(Q,t,T), \qquad (17)$$

where the prefactor, $A(Q,T)$, is an amendment of the conventional model due to peculiarities of the NSE experiment. It contains possible further dynamics (relaxation or vibrational), which are faster than the lower time limit of the NSE experiment (20 ps). Due to the uncertainty of how these dynamics vary the amplitude in the concrete situation, e.g., polarization efficiency, detector efficiency at high neutron energies, the factor has to be fitted for each combination of Q and T separately. In all cases, the plateau value of $S(Q,t)$ could be observed reliably in the NSE window. Therefore, the uncertainty of $A(Q,T)$ ranges from 1% to 3%. The ensuing uncertainty in the relaxation times has been considered in the error calculation. The assumption of two independent relaxation mechanisms is justified by the data shown in Fig. 5.

As shown in Fig. 5, the fit with only the α-relaxation is not appropriate for the combination of the lowest temperature $T = 220$ K with the highest $Q = 1.6$ Å^{-1}. It rather seems that there is an additional relaxation step around 200 ps. In retrospect, this is not surprising because earlier (conventional) QENS experiments have revealed a relaxation of the methyl group (MG).[47] It could be described by a three-site jump motion of the hydrogen atoms in the methyl group

$$S_{\mathrm{MG}}(Q,t,T) = \frac{5}{8} + \frac{3}{8}[A_0(Q) + (1 - A_0(Q)) \cdot \phi(t)] \qquad (18)$$

with the elastic incoherent structure factor (EISF)

$$A_0(Q) = \frac{1}{3} \cdot \left(1 + 2 \cdot \frac{\sin(Qd_{\mathrm{HH}})}{Qd_{\mathrm{HH}}}\right), \qquad (19)$$

where $d_{\mathrm{HH}} = 1.78$ Å as the H-H distance in the methyl group, and a distribution of Debye relaxations

$$\phi(t) = \int_0^\infty \exp\left(-\frac{t}{\tau_{\mathrm{MG}}^0 \exp(E_{\mathrm{A}}/k_{\mathrm{B}}T)}\right) \cdot g(E_{\mathrm{A}}) \cdot dE_{\mathrm{A}} \qquad (20)$$

resulting from a normal distribution of energy barriers, where

$$g(E_{\mathrm{A}}) = \frac{1}{\sqrt{2\pi} \cdot \Delta E_{\mathrm{A}}} \exp\left(\frac{(E_{\mathrm{A}} - E_{\mathrm{A}}^0)^2}{2\Delta E_{\mathrm{A}}^2}\right). \qquad (21)$$

The model parameters for propylene glycol, ${\tau_{\mathrm{MG}}}^0 = 5.8 \times 10^{-15}$ s, ${E_{\mathrm{A}}}^0 = 2273 k_{\mathrm{B}}$ K, $\Delta E_{\mathrm{A}} = 311 k_{\mathrm{B}}$ K were all taken from Ref. 47 and not fitted from the data here. Therefore, the introduction of the methyl group rotation term does not induce any additional uncertainty in the determination of the α-relaxation times. It only changes the values at low temperature slightly.

Except for the methyl group rotation, which is substantiated by Ref. 47, we do not consider other internal modes

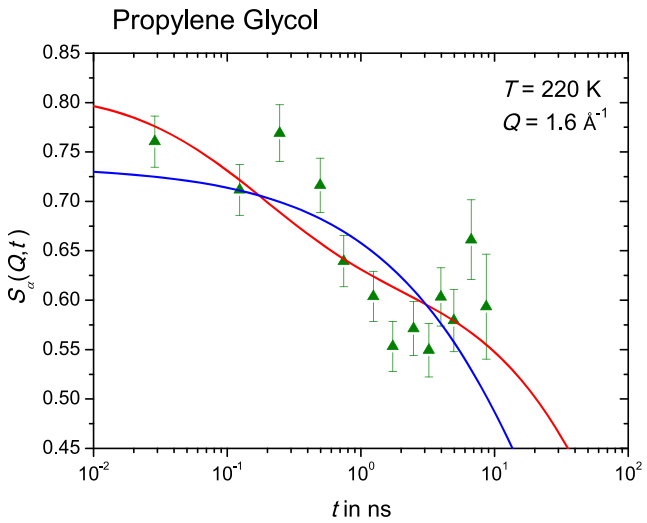

FIG. 5. Fit of NSE data of propylene glycol at low temperature, $T = 220$ K, and high scattering vector, $Q = 1.6$ Å^{-1}. Blue: fit with α-relaxation only, red: fit with methyl group rotation + α-relaxation.

neither a rotation of the molecule as a whole. We assume that these motions are sterically hindered so that they do not play a role in the observed time range.

IV. RESULTS

A. Incoherent neutron spin echo spectroscopy

Fig. 6(a) shows the α-relaxation incoherent intermediate scattering function, $S_\alpha(Q,t)$ for polystyrene, measured by neutron spin echo at wave vectors $Q = 0.15$ Å^{-1}, $Q = 0.25$ Å^{-1}, $Q = 0.4$ Å^{-1}, $Q = 0.6$ Å^{-1}, and $Q = 0.8$ Å^{-1} for different temperatures from 390 K to 455 K, while Fig. 6(b) shows the same for propylene glycol at $Q = 0.6$ Å^{-1}, $Q = 1.0$ Å^{-1}, and $Q = 1.6$ Å^{-1} for different temperatures from 220 K to 250 K.

For polystyrene, the *complete* incoherent intermediate scattering function was fitted by the usual Kohlrausch function

$$S_\alpha(Q,t) = A(Q,T) \cdot \exp[-(t/\tau_K(Q,T))^\beta], \qquad (22)$$

where the Kohlrausch characteristic time, τ_K, was fitted individually for each combination of scattering vector and temperature, while the Kohlrausch exponent was fitted for all combinations of Q and T as a single value, $\beta = 0.70 \pm 0.06$. The prefactors $A(Q,T)$ had to be left free because of residual contributions of coherently scattered neutrons (instrumental background). In order to demonstrate the accuracy of the Kohlrausch function fit to the NSE data for polystyrene and propylene glycol, each individual $S_\alpha(Q,t)$ and its fit curves are presented in the supplementary material. The residuals for the NSE data and its Kohlrausch function fit are also presented, where it shows scattering around zero, except for large time, t, which accounts for a systematic deviation.

Fig. 12(a) below shows the resulting time constants for polystyrene for $Q = 0.8$ Å^{-1} (in the case of 455 K as the extrapolated value) in comparison to data from non-Q-resolving methods.[5] The offset by about one decade is not surprising because the NSE relaxation times can be shifted by adjusting Q. What is more disturbing is that the temperature dependence is much weaker than expected for the α-relaxation and rather Arrhenius-like. Already during the experiment, it became clear that a decay of $S_\alpha(Q,t)$ could be observed at unexpectedly low temperatures, like 390 K and 410 K. This seems to indicate that in this experiment, $S_\alpha(Q,t)$ is predominantly influenced by a secondary relaxation, except maybe for the two highest temperatures, 420 K and 455 K. We suspect that the origin of the secondary relaxation is a motion of the phenyl rings but could not identify the exact mechanism of motion. Due to that (unexpected) result, the evaluation of the polystyrene data towards a cooperativity length was not continued. Therefore, no comparison with the calorimetric data is possible.

For propylene glycol, the α-relaxation part of the incoherent intermediate scattering function is described by the usual Kohlrausch function, shown in Equation (22) with $A(Q,T) = 1$. The function was combined with the methyl group contribution and the fast processes, as described by Equations (17)–(21). As for polystyrene, the Kohlrausch characteristic time, τ_K, was fitted individually for each combination of scattering vector and temperature, while the Kohlrausch exponent was fitted for all combinations of Q and T as $\beta = 0.69 \pm 0.04$.

It can be seen that the fit function describes the data well. Fig. 11 shows the resulting Kohlrausch times, τ_K, depending on the temperature and the scattering vector, Q. In the double logarithmic representation, the points fall on straight lines indicating that $\tau_K(Q)$ follows a power law

$$\tau_K(Q,T) = \text{const}(T) \cdot Q^{-n} \qquad (23)$$

with $n = 2.67 \pm 0.11$. In passing, we note that $n \cdot \beta = 1.85 \pm 0.13$. This value is marginally smaller than 2, indicating a violation of Gaussianity, as it was observed for polyisoprene in the range $Q > 1$ Å^{-1}.[48]

The resulting Kohlrausch times, τ_K, depending on the temperature and the scattering vector, Q, obtained from the Kohlrausch function fit are presented in Fig. 11, where straight lines for each temperature are indicated as described above. With the relaxation times at the same temperatures determined from AC calorimetry, τ_K^{AC}, the corresponding scattering vector, Q^*, and subsequently cooperativity length, l, and volume, V, can be obtained for comparison, as will be discussed Section IV C.

B. AC calorimetry

AC calorimetric temperature scans at constant frequency were performed in the vicinity of the glass transition. The

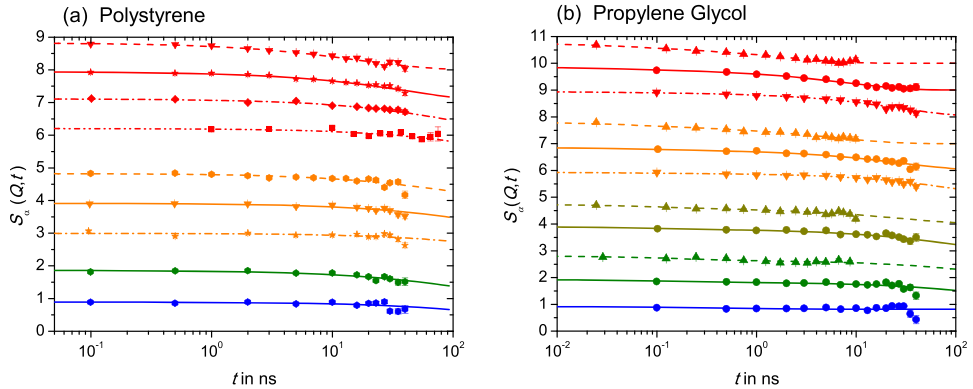

FIG. 6. Synopsis of fits of the NSE data. Data points and fit curves are offset vertically to avoid crowding. Temperatures are indicated with colors (bottom to top) and scattering vectors Q with symbols. (a) Polystyrene: 390 K (blue), 410 K (green), 420 K (orange), and 455 K (red), with 0.15 Å^{-1} (squares), 0.25 Å^{-1} (diamonds), 0.4 Å^{-1} (stars), 0.6 Å^{-1} (triangles down), and 0.8 Å^{-1} (hexagonals). (b) Propylene glycol: 200 K (blue), 220 K (green), 230 K (dark yellow), 240 K (orange), and 250 K (red), with symbols: 0.6 Å^{-1} (triangles down), 1.0 Å^{-1} (circles), and 1.6 Å^{-1} (triangles up). See the supplementary material for more details.

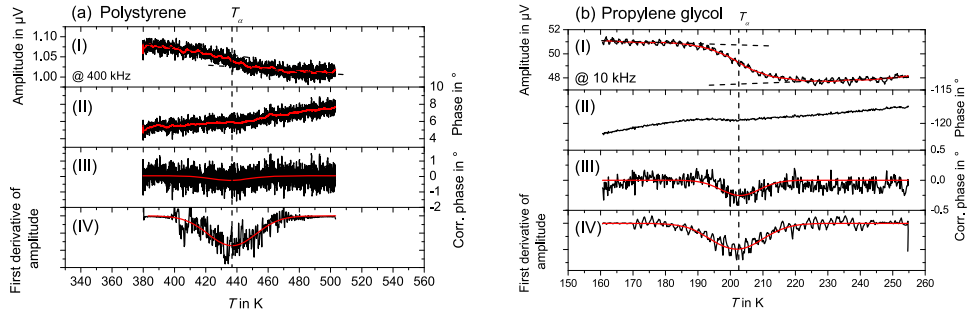

FIG. 7. Laser-modulated AC calorimetric measurement in the temperature range of the glass transition of (a) polystyrene at 400 kHz and (b) propylene glycol at frequency 10 kHz. (I) Thermocouple voltage amplitude, (II) phase angle between oscillator voltage and thermocouple voltage, (III) corrected phase angle, and (IV) first derivative of the thermocouple voltage amplitude with fitted Gaussian function. The maximum is the dynamic glass transition temperature, T_α(400 kHz), for polystyrene and T_α(10 kHz) for propylene glycol.

amplitude of the thermocouple signal shows a step at the glass transition and the phase angle between power and temperature oscillation shows a peak (Fig. 7). The phase angle was corrected for the influence of the changing heat capacity at the glass transition as described in Ref. 49.

For direct comparison of the temperature position and the shape of the measured signals, we normalized all curves by subtracting the tangent to the values measured below the dynamic glass transition and dividing the remaining curves by the tangent above the dynamic glass transition. Fig. 8 shows the resulting normalized heat capacity curves. The first order derivatives of the normalized curves are fitted with a Gaussian function, in order to determine the full width at half maximum of the transition, FWHM = $2\delta T$, as shown in Fig. 9. Besides the shift of T_α by about 90 K for polystyrene and about 40 K for propylene glycol, a significant broadening of the dynamic glass transition with increasing frequency is seen in Figs. 8 and 9.

The dynamic glass transition temperatures T_α from the laser-modulated AC calorimeter together with data from other calorimetric methods and dielectric spectroscopy are plotted in the relaxation map in Fig. 12 below. The VFT from the dielectric data, shown as solid black line, fits the results from AC and laser-modulated calorimetry too.

The δT, which is half of the full width at half maximum (FWHM) of the Gaussian fits, FWHM = $2\delta T$, is shown in Fig. 10(I), while the resulting characteristic lengths considering energy fluctuation (δT = 0; Equation (1)), and considering temperature fluctuation (δT; Equation (2)), are plotted in Fig. 10(II). For the calculation, the glass transition temperature and half of FWHM of the transition were determined from AC calorimetry measurements, shown in Fig. 9, and heat capacities were taken from Fig. 1. Experimentally derived and calculated parameters determined from averaged AC calorimetry measurements for polystyrene and propylene glycol are presented in Table I.

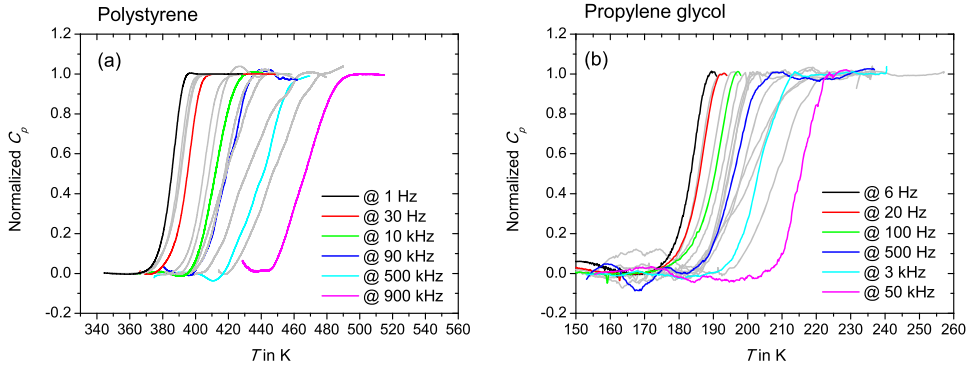

FIG. 8. Normalized heat capacity (reciprocal product of thermocouple voltage amplitude times frequency) at the dynamic glass transition for different frequencies for (a) polystyrene[28] and (b) propylene glycol. Reproduced with permission from Chua *et al.*, Colloid Polym. Sci. **292**, 1893 (2014). Copyright 2014 Springer.

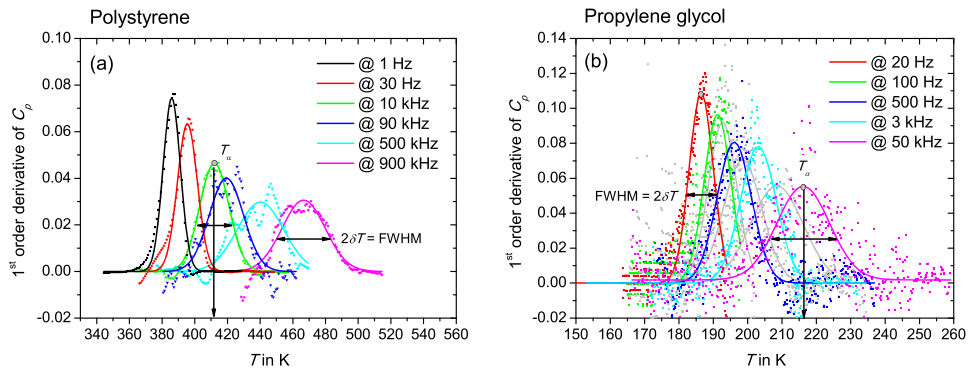

FIG. 9. First order derivative of the heat capacity for different frequencies, and fitted with the Gaussian fit function. The dynamic glass transition temperature and the full width half maximum (FWHM) are labelled as T_α and FWHM = $2\delta T$, respectively.

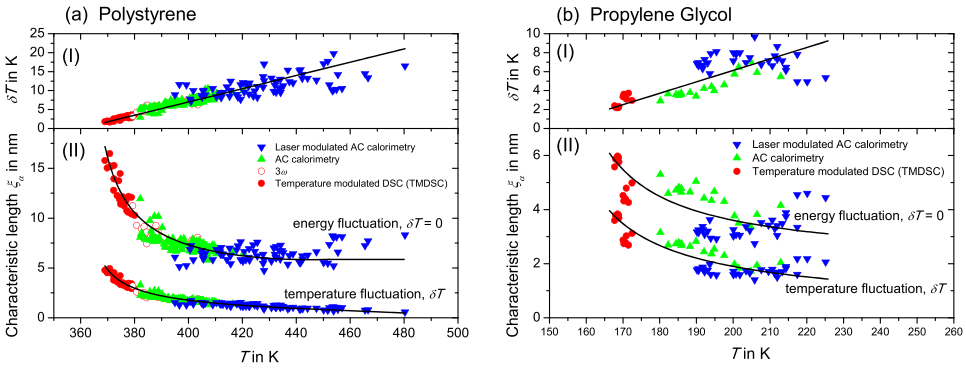

FIG. 10. (I) δT, half of FWHM of the glass transition for (a) polystyrene[28] and (b) propylene glycol, respectively, which is determined from the Gaussian fit of the first derivation of heat capacity curves. (II) The corresponding characteristic lengths, ξ_α, are determined (top) considering energy fluctuation, $\delta T = 0$, with Equation (1) and (bottom) considering temperature fluctuation, δT, with Equation (2). The solid black line for δT is average fit, which is subsequently calculated for solid black lines for $\xi_\alpha(\delta T = 0)$ and $\xi_\alpha(\delta T)$.

For propylene glycol, for which reliable NSE data for the α-relaxation are available, the cooperativity length scales considering temperature fluctuations (δT; Equation (2)) and neglecting temperature fluctuations ($\delta T = 0$; Equation (1)) differ only by a factor of two, making comparison with the NSE derived length scale difficult. On the other hand for polystyrene, the two values differ by a factor of 6, which would allow better comparison with the NSE derived length scale, if reliable NSE data for the α-relaxation would be available.

C. Combination of NSE and AC calorimetric data

With neutron spin echo for propylene glycol, the normalized intermediate scattering function $S_{\text{inc}}(Q,t)$ at fixed scattering wave vectors of Q = 1.0 Å^{-1} and Q = 1.6 Å^{-1} for temperatures of 220 K, 230 K, 240 K, and 250 K, and for the temperatures of 240 K and 250 K with additional measurement for Q = 0.6 Å^{-1} is available. The resulting Kohlrausch times, τ_K, for the corresponding temperature and scattering vector Q determined from Equation (22) with NSE data are illustrated in Fig. 11 as solid symbols. Each solid line represents the power law dependence (Equation (23)) for a temperature from 220 K to 250 K. They all have the same slope, which means that the exponent n was considered temperature independent.

Comparison between the length scales determined with Equations (1) or (2) and the cooperativity length derived from the NSE data for the same temperature requires comparable time scales for both data. Due to the high frequency AC calorimetry and the comparable low frequency NSE data, we have a certain overlapping time range allowing such direct comparison. With the $\tau_K{}^{AC} = 0.83/\omega_{max}$ (horizontal dashed lines), the corresponding Q^* and l (vertical dashed lines) can be determined, via the intersections with solid lines or using Equation (23) for each temperature. The neutron scattering based cooperativity length, l, is calculated with $l = 4.47/Q^*$ as in Equation (11).

The results are shown in Table II. The error estimates are based on two sources: (i) the errors of the constant and the exponent n in Equation (23) resulting from the least-square fit, (ii) the error in ω_{max} resulting from the fit of the AC calorimetry curves. The values from 230 K were unavailable from AC calorimetry and therefore replaced by an extrapolation from 220 K using the VFT Equation (14). (For this temperature, no error estimate is given because the uncertainty of the extrapolation cannot be judged.)

Finally the calculated cooperativity length and volume from neutron scattering, l and V, in Table II are compared

TABLE I. Experimentally derived and calculated parameters for (a) polystyrene and (b) propylene glycol: characteristic frequency, ω_{max}, specific heat capacity of glass and liquid, $c_v{}^{glass}$ and $c_v{}^{liquid}$, half-width, δT for respective temperature determined from averaged AC calorimetry measurements based on solid black line in Fig. 10(I), and characteristic length and volume, ξ_α, and V_α, calculated based on Equations (1) and (2), for energy fluctuation, $\delta T = 0$, and temperature fluctuation, δT, respectively.

(a) Polystyrene – AC calorimetry								
T (K)	ω_{max} (rad s^{-1})	$c_p{}^{glass}$ (J/mol·K)	$c_p{}^{liquid}$ (J/mol·K)	δT(K)	$\xi_\alpha(\delta T = 0)$(nm)	$\xi_\alpha(\delta T)$(nm)	$V_\alpha(\delta T = 0)$(nm^3)	$V_\alpha(\delta T)$(nm^3)
390	128	169.8	194.0	5.2	8.44	2.20	314.8	5.59
400	2 900	174.6	196.6	7.0	7.32	1.76	205.1	2.88
410	27 500	179.4	199.9	8.7	6.64	1.47	153.5	1.67
420	1 47 000	184.2	201.6	10.5	6.22	1.25	126.2	1.03
430	5 42 000	189.0	204.2	12.2	5.97	1.08	111.5	0.67
440	1 500 000	193.7	206.7	14.0	5.85	0.94	104.9	0.44
450	3 600 000	198.5	209.2	15.7	5.85	0.82	104.9	0.29
455	5 200 000	200.9	210.5	16.6	5.90	0.76	107.5	0.23
(b) Propylene glycol – AC calorimetry								
T (K)	ω_{max} (rad s^{-1})	$c_v{}^{glass}$ (J/mol·K)	$c_v{}^{liquid}$ (J/mol·K)	δT(K)	$\xi_\alpha(\delta T = 0)$(nm)	$\xi_\alpha(\delta T)$(nm)	$V_\alpha(\delta T = 0)$(nm^3)	$V_\alpha(\delta T)$ (nm^3)
190	548	90.8	138.0	5.1	3.85	2.17	29.9	5.3
200	10 900	94.8	139.1	6.3	3.53	1.87	23.0	3.4
210	1 18 000	98.8	140.7	7.5	3.30	1.66	18.8	2.4
220	8 19 000	102.8	142.8	8.7	3.13	1.49	16.1	1.7

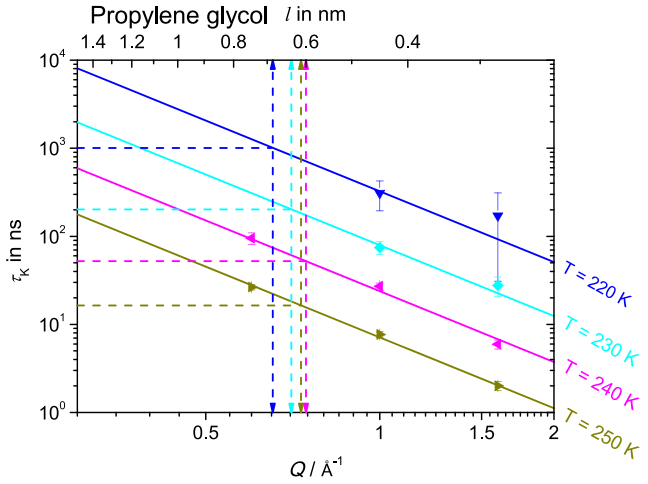

FIG. 11. The neutron scattering vector, Q, with its corresponding time constant, τ_K, according to Equation (23) as solid symbols for propylene glycol. Solid lines are linear fits with the same slope for each temperature. Dashed horizontal lines are $\tau_K{}^{AC}$ at respective temperature, in order to determine the corresponding Q^* and l according to Equation (11). The values are shown in Table II.

with the characteristic length and volume from AC calorimetry, ξ_α and V_α, in Table I for each temperature. The results are summarized in Fig. 13.

V. DISCUSSION

As shown in the relaxation map in Fig. 12, the frequency dependence of the calorimetric dynamic glass transition temperatures of polystyrene and propylene glycol measured with different calorimetric devices indicates consistency and coincides with the dielectric relaxation data.[31–33] The laser-modulated AC calorimeter proved to be a reliable device to measure dynamic glass transition up to high frequency range.

From AC calorimetry measurements characteristic lengths, ξ_α, are calculated based on Equations (1) and (2), by neglecting and taking into account temperature fluctuations, respectively. In order to calculate the characteristic length, the CRR is taken as a sphere where the characteristic length is the diameter of the sphere, and the c_p is converted to c_v. On the other hand from neutron scattering measurements, the cooperativity length, l as spherical diameter is determined based on the Kohlrausch time, $\tau_K{}^{AC} = 0.83/\omega_{max}$. These results from AC calorimetry (solid blue triangles for energy fluctuation and solid red circles for temperature fluctuation) and QENS (solid green diamonds) are depicted in Fig. 13 for comparison.

TABLE II. Calculation of the co-operativity length for propylene glycol from dynamic neutron scattering based on Fig. 11. ω_{max} is the maximum position in the imaginary part of the dynamic heat capacity, $\tau_K{}^{AC}$ is the equivalent Kohlrausch time which is calculated from $\omega_{max} = 0.83/\tau_K{}^{AC}$, Q^* is the scattering vector at which the Kohlrausch time of the NSE experiment coincides with the latter, l is the cooperativity length calculated as spherical diameter, and V the cooperativity volume.

	Propylene glycol – QENS				
T (K)	ω_{max} (rad s^{-1})	$\tau_K{}^{AC}$ (ns)	Q^* (Å^{-1})	l (nm)	V (nm^3)
220	8 19 000	1009	0.65	0.68	0.17
230	4 086 000	203	0.70	0.64	0.13
240	15 800 000	52	0.74	0.60	0.11
250	50 400 000	16	0.73	0.61	0.12

The cooperativity length from QENS, l, is about a factor of three smaller than the calculated characteristic length from AC calorimetry, ξ_α, by consideration of temperature fluctuations. The calculated characteristic length considering energy fluctuation only yields values, which are about 5 times larger than l at 220 K, where an overlap between QENS and AC calorimetry is realized. On the other hand, in order to check to what extent this result depends on the choice of the shape of the cooperativity volume as a sphere, here we repeat the calculation of Section II assuming the shape of CRR as a cube and ξ_α as the edge length a. Then the radius of gyration is $R_g{}^2 = a^2/4$, which leads to

$$l = \frac{\sqrt{12}}{Q^*} = \frac{3.464}{Q^*}. \tag{24}$$

Comparing this to Equation (11), it seems that there is an additional uncertainty in the comparison because this value is smaller by 23%. But one has to take into account that the change of the assumption of the shape of the cooperativity

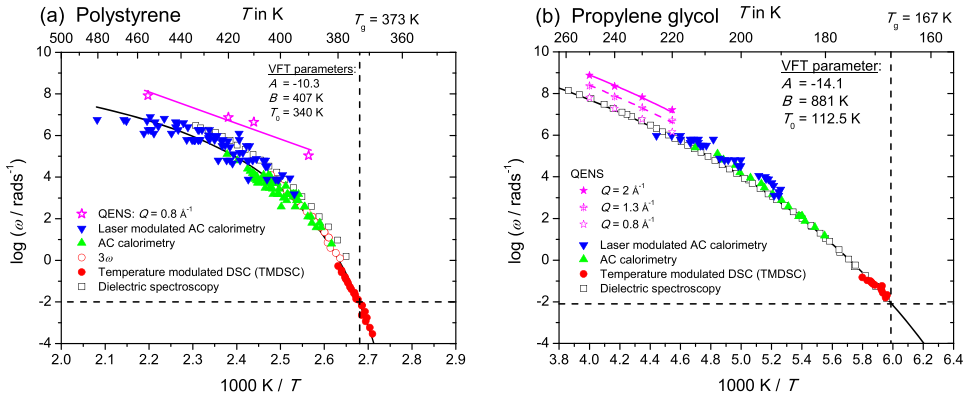

FIG. 12. Relaxation map for (a) polystyrene[28] and (b) propylene glycol, showing data from different calorimetric devices, from dielectric spectroscopy,[31–33] as empty black squares, and from AC and laser-modulated calorimetry measured in this work as solid symbols. The solid black lines are the VFT fits, based on Equation (14), with parameters listed. The empty magenta stars denote the QENS relaxation times with Q indicated in the legend. These points from QENS deviate significantly from the VFT curve for polystyrene, while they follow closely the expected trend for propylene glycol.

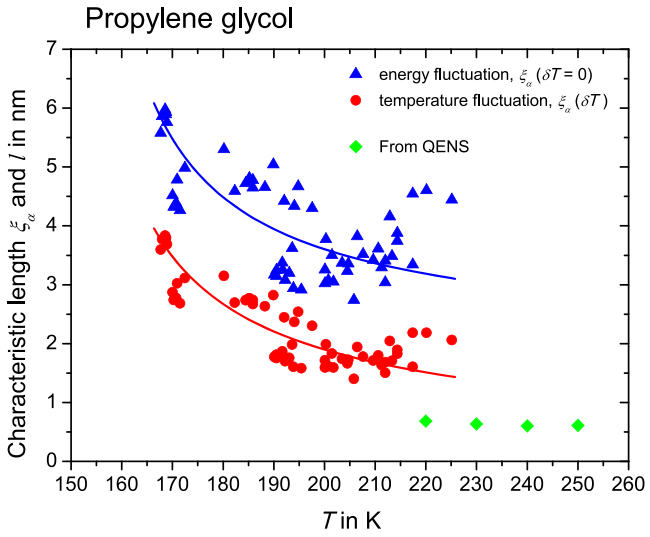

FIG. 13. Data for propylene glycol from Fig. 10(II) and cooperativity length, l as spherical diameter (solid green diamonds) determined from dynamic neutron scattering, with $l = 4.47/Q^*$ (Equation (11)) and $\omega_{max} = 0.83/\tau_K{}^{AC}$ (Equation (13)).

volume also implies a change of the definition of ξ_α in Equation (3), which partially compensates this uncertainty. With the cooperativity volume as a cube, the characteristic length is about 20% smaller in comparison to ξ_α in Equation (3).

What is effectively compared is the volume of the cooperatively rearranging unit. Based on that, one obtains

$$V_\alpha = \frac{24\sqrt{3}}{Q^{*3}} = \frac{41.569}{Q^{*3}} \tag{25}$$

for the cube, which is about 12% smaller as compared to the spherical case in Equation (9).

One can see that the different choice of the shape only leads to a 12% change of the volume. The reason is that going to a less compact shape increases the R_g, but on the other hand increases the volume too, so that both effects partially compensate. The shape-related uncertainty in volume corresponds to an uncertainty of 4% in Q^*, which is clearly below the experimental accuracy. In addition, a different choice of the characteristic length with respect to the shape (e.g., the diagonal in case of the cube) would lead to a change of the equation defining ξ_α (Equation (3)) but not the comparison between the cooperative volume V_α and Q^*. Because the sphere has the smallest radius of gyration at a given volume,[50] Equation (11) gives the maximum possible factor in the inverse proportional relation between ξ_α and Q^*. Concluding, we have to admit that there is a significant definition-dependence in ξ_α but this will not affect the decision between the different expressions for the cooperativity on grounds of neutron scattering data.

Even with the consideration of different geometries of the CRR, the general conclusion of the results remains unaffected because the characteristic length, ξ_α, from AC calorimetry from Equation (2) by considering temperature fluctuation is significantly closer to the cooperativity length l from QENS, which is almost 5 times smaller than the characteristic length obtained from Equation (1) assuming there is no temperature fluctuation. Nevertheless, the difference between the characteristic length, ξ_α, from AC calorimetry by considering temperature fluctuation and cooperativity length, l, from QENS cannot be disregarded. Further investigations are needed to clarify this difference.

VI. CONCLUSIONS

For polystyrene, unexpectedly, a secondary relaxation was present in the time-temperature range where the comparison to AC calorimetry was supposed to take place. Therefore, no reliable comparison of the cooperativity length could be done for polystyrene.

Propylene glycol has been widely investigated to show no indication of a secondary relaxation, neither from macroscopic experiments[51] nor from quasielastic neutron scattering.[47] The absence of secondary relaxation is essential to ensure that the result from the measurements is the α-relaxation, especially for quasielastic neutron scattering.

The cooperativity length derived from AC calorimetry and QENS provides better agreement based on temperature fluctuations, than based on energy fluctuations. However, an exact equality could not be found, which is not surprising in view of the uncertainties in the definition of the characteristic length.

This allows the following preliminary conclusions: (i) At the same temperature of 220 K and the same time scale of τ_K ca. 1 μs, both independent methods with AC calorimetry and QENS yield characteristic length scales close to one nm. By this, the existence of a characteristic length scale for the cooperative motions relevant for the glass transition is supported. (ii) Furthermore since the estimate of this characteristic length scale *considering temperature fluctuations* provides a much better match between the length scales from AC calorimetry and QENS, the existence of temperature fluctuations in nanoscale subsystems is supported.

To obtain more definite answers to these long outstanding questions, the approaches as presented in this work by comparing the length scales from AC calorimetry and QENS should be continued with the guidelines: (i) A material should be chosen where the difference between the cooperativity values considering energy and temperature fluctuations (Equations (1) and (2)) is larger. This would enable one to make an unambiguous decision in spite of the factor 3 difference between both experimental methods to derive the cooperativity length. (ii) The material must not have any disturbing relaxation in the range of the α-relaxation in the QENS experiments as propylene glycol. (iii) The overlap of temperatures and time scales should be large as for polystyrene.

SUPPLEMENTARY MATERIAL

See supplementary material for Kohlrausch function fits to the NSE data for each polystyrene and propylene glycol measurement. The individual $S_\alpha(Q,t)$, its fit curves, and the residuals are presented.

ACKNOWLEDGMENTS

The authors thank R. Richert, Tempe, for providing the dielectric relaxation data of propylene glycol and useful discussion. We also thank D. Richter, Jülich, for his encouragement to pursue this work.

[1] R. Kubo, *Statistical Mechanics: An Advanced Course with Problems and Solutions* (North-Holland, Amsterdam, 1965).
[2] R. Kubo, *Thermodynamics: An Advanced Course with Problems and Solutions* (North-Holland, Amsterdam, 1968).
[3] C. Kittel, *Thermal Physics* (Wiley, New York, 1969).
[4] L. D. Landau and E. M. Lifshitz, *Statistical Physics* (Akademie-Verlag, Berlin, 1987).
[5] G. S. Boltachev and J. W. P. Schmelzer, J. Chem. Phys. **133**(13), 134509–134511 (2010).
[6] E. Donth, *Glass Transition* (Springer, Berlin, 2001).
[7] C. Kittel, Phys. Today **41**(5), 93 (1988).
[8] B. B. Mandelbrot, Phys. Today **42**(1), 71–73 (1989).
[9] R. McFee, Am. J. Phys. **41**(2), 230–234 (1973).
[10] R. McFee, Am. J. Phys. **41**, 1212 (1973).
[11] M. von Laue, Phys. Z. **18**, 542–544 (1917).
[12] C. Kittel, Am. J. Phys. **41**(10), 1211–1212 (1973).
[13] J. W. Gibbs, *Elementare Grundlagen der Statistischen Mechanik* (Johann Ambrosius Barth, Leipzig, 1905).
[14] E. Donth, *Glasübergang* (Akademie-Verlag, Berlin, 1981).
[15] E. Donth, E. Hempel, and C. Schick, J. Phys.: Condens. Matter **12**, L281–L286 (2000).
[16] E. Donth, Eur. Phys. J. E: Soft Matter **12**(1), 11–18 (2003).
[17] E. Donth, J. Non-Cryst. Solids **53**(3), 325–330 (1982).
[18] S. Karmakar, C. Dasgupta, and S. Sastry, Proc. Natl. Acad. Sci. U. S. A. **106**(10), 3675–3679 (2009).
[19] S. Albert, T. Bauer, M. Michl, G. Biroli, J.-P. Bouchaud, A. Loidl, P. Lunkenheimer, R. Tourbot, C. Wiertel-Gasquet, and F. Ladieu, Science **352**(6291), 1308–1311 (2016).
[20] R. Casalini, D. Fragiadakis, and C. M. Roland, J. Chem. Phys. **142**(6), 064504 (2015).
[21] J. W. Gibbs, *The Collected Works* (Longmans, Green and Co., Toronto, New York, London, 1928).
[22] J. D. van der Waals, Z. Phys. Chem. **13**, 657 (1894).
[23] T. L. Hill, *Thermodynamics of Small Systems* (Dover Publications, Mineola, NY, USA, 2002).
[24] E. Donth, W. Schenk, and A. Ebert, Acta Polym. **30**(9), 540–546 (1979).
[25] H. Sillescu, Acta Polym. **45**, 2 (1994).
[26] J. M. O'Reilly, Crit. Rev. Solid State Mater. Sci. **13**(3), 259–277 (1987).
[27] C. T. Moynihan, J. Am. Ceram. Soc. **76**(5), 1081–1087 (1993).
[28] Y. Z. Chua, G. Schulz, E. Shoifet, H. Huth, R. Zorn, J. W. P. Schmelzer, and C. Schick, Colloid Polym. Sci. **292**, 1893–1904 (2014).
[29] O. Glatter in *Neutrons, X-rays and Light: Scattering Methods Applied to Soft Condensed Matter*, edited by T. Zemb and P. Lindner (Elsevier, Amsterdam, 2002), pp. 110.
[30] J. Colmenero, A. Arbe, and A. Alegria, J. Non-Cryst. Solids **172-174**(1), 126–137 (1994).
[31] S. Weinstein and R. Richert, Phys. Rev. B **75**, 064302 (2007).
[32] F. J. Stickel, PhD thesis, University of Mainz, *Untersuchung der Dynamik in niedermolekularen Flüssigkeiten mit Dielektrischer Spektroskopie* (Shaker Verlag, Aachen, 1995).
[33] N. Hao, M. Bohning, and A. Schönhals, Macromolecules **40**, 9672–9679 (2007).
[34] C. A. Angell and D. L. Smith, J. Phys. Chem. **86**(19), 3845–3852 (1982).
[35] U. Gaur and B. Wunderlich, J. Phys. Chem. Ref. Data **11**(2), 313–325 (1982).
[36] G. S. Parks and H. M. Huffmann, J. Phys. Chem. **31**(12), 1842–1855 (1927).
[37] L. Singh, P. J. Ludovice, and C. L. Henderson, Thin Solid Films **449**, 231–241 (2004).
[38] S. Takahara, M. Ishikawa, O. Yamamuro, and T. Matsuo, J. Phys. Chem. B **103**, 792–796 (1999).
[39] D. R. Lide, *CRC, Handbook of Chemistry and Physics*, 85th ed. (CRC Press, 2004).
[40] E. Shoifet, Y. Z. Chua, H. Huth, and C. Schick, Rev. Sci. Instrum. **84**(7), 073903–073912 (2013).
[41] A. W. van Herwaarden, Thermochim. Acta **432**(2), 192–201 (2005).
[42] R. Jakobi, E. Gmelin, and K. Ripka, J. Therm. Anal. **40**(3), 871–876 (1993).
[43] E. Shoifet, G. Schulz, and C. Schick, Thermochim. Acta **603**, 227–236 (2015).
[44] F. Mezei, *Neutron Spin Echo*, Lecture Notes in Physics, Vol. 128 (Springer, Berlin, 1980).
[45] M. Bée, *Quasielastic Neutron Scattering: Principles and Applications in Solid State Chemistry, Biology and Materials Science* (Adam Hilger, Bristol, 1988).
[46] O. Holderer, M. Monkenbusch, R. Schätzler, H. Kleines, W. Westerhausen, and D. Richter, Meas. Sci. Technol. **19**, 034022 (2008).
[47] R. Zorn, M. Mayorova, D. Richter, A. Schonhals, L. Hartmann, F. Kremer, and B. Frick, AIP Conf. Proc. **982**(1), 79–84 (2008).
[48] A. Arbe, J. Colmenero, F. Alvarez, M. Monkenbusch, D. Richter, B. Farago, and B. Frick, Phys. Rev. E **67**(5), 051802 (2003).
[49] S. Weyer, A. Hensel, J. Korus, E. Donth, and C. Schick, Thermochim. Acta **304-305**, 251–255 (1997).
[50] S. J. Leach, *Physical Principles and Techniques of Protein Chemistry* (Academic Press, New York, 1973).
[51] N. O. Birge, Phys. Rev. B **34**(3), 1631–1642 (1986).